

Article

Optimization of Calcination Conditions for Cu/ZnO/Al₂O₃-ZrO₂ Catalyst

Nur Insyirah Zulkifli ¹, Nor Hafizah Berahim ¹, Noor Asmawati Mohd Zabidi ^{1,*}  and Sara Faiz Hanna Tasfy ²

¹ Department of Fundamental and Applied Sciences, Universiti Teknologi PETRONAS, Seri Iskandar 32610, Malaysia; nur_19000323@utp.edu.my (N.I.Z.); nor_19001638@utp.edu.my (N.H.B.)

² Department of Chemical and Petroleum Engineering, American University of Ras Al Khaimah, Ras Al Khaimah 10021, United Arab Emirates; sara.tasfy@aurak.ac.ae

* Correspondence: noorasmawati_mzabidi@utp.edu.my; Tel.: +60-5-368-7675

Abstract: Promoted Cu/ZnO catalyst was synthesized on Al₂O₃-ZrO₂ support. Effects of calcination conditions on the catalytic performance in a CO₂ hydrogenation reaction were studied systematically using the response surface methodology (RSM). The application of RSM with rotatable central composite design (RCCD) for optimization on the influence of catalyst's calcination variables on the CO₂ conversion and methanol selectivity is presented. The calcination variables studied include temperature, A (181–518 °C), ramping rate, B (1–30 °C/min), and duration, C (1–7 h). From the RSM-generated model, the optimum calcination condition for this catalyst was 350 °C with 17.5 °C/min ramping rate for a 4 h duration. At the optimum calcination condition, the catalyst exhibited a Brunauer–Emmett–Teller (BET) surface area of 147 m²/g, a pore volume of 0.31 cm³/g, and a pore diameter of 8.1 nm.

Keywords: RSM; CO₂ hydrogenation; methanol synthesis; calcination condition; Cu-based catalyst



Citation: Zulkifli, N.I.; Berahim, N.H.; Mohd Zabidi, N.A.; Tasfy, S.F.H. Optimization of Calcination Conditions for Cu/ZnO/Al₂O₃-ZrO₂ Catalyst. *Catalysts* **2021**, *11*, 871. <https://doi.org/10.3390/catal11080871>

Academic Editor: Mingyuan Zheng

Received: 25 June 2021

Accepted: 16 July 2021

Published: 21 July 2021

Publisher's Note: MDPI stays neutral with regard to jurisdictional claims in published maps and institutional affiliations.



Copyright: © 2021 by the authors. Licensee MDPI, Basel, Switzerland. This article is an open access article distributed under the terms and conditions of the Creative Commons Attribution (CC BY) license (<https://creativecommons.org/licenses/by/4.0/>).

1. Introduction

The hydrogenation of CO₂ into value-added products such as methanol and dimethyl ether (DME) is one of the attractive options to mitigate the rise in CO₂ concentration in the atmosphere [1–5]. Cu-based catalysts have been recognized as efficient catalysts for the industrial methanol production that uses syngas as the feedstock. Methanol production based on CO₂ feedstock is yet to be applied at industrial scale, despite the extensive research conducted in this field. Some of the issues on the CO₂ hydrogenation process relates to the co-production of H₂O with methanol which would have detrimental effects on the conventional Cu-based catalyst. It was reported by [6–8] that the Cu/ZnO catalyst was deactivated due to accelerated crystallization of Cu and ZnO by water produced from CO₂-rich feedstock used in the methanol synthesis. Thus, intense efforts on catalyst design for methanol synthesis via CO₂ hydrogenation route have been carried out by many researchers around the world [9–13]. Some of the catalyst design approach include introduction of multicomponent system which has the capability to activate the very stable CO₂ molecule and dissociate H₂ molecule, and to minimize the effects of H₂O on the physicochemical properties of the catalyst [6].

Methanol synthesis is a structure-sensitive reaction, thus the efficiency of the catalyst is significantly influenced by the method of preparation of the catalyst, their pre-treatment conditions, active metals component, and choice of support and promoters. The preparation methods for the methanol synthesis catalysts include impregnation, co-precipitation, combustion, and sol-gel [7]. The industrial methanol catalyst is typically prepared using the co-precipitation method. Fujita et al. [14] investigated the effects of calcination and reduction conditions on the physicochemical properties of Cu/ZnO catalyst prepared by the co-precipitation method. They reported that the crystallite size of CuO for a catalyst prepared from aurichalcite precursor was significantly affected by the ramping rate during

the calcination process. The crystallite size of CuO was found to increase from 3.9 nm to 8.5 nm when the ramping rate was increased from 5 K/min to 100 K/min. The increase in the ramping rate during the calcination process resulted in a decrease in Cu dispersion and a corresponding decrease in the rate of methanol formation.

The commonly used γ -Al₂O₃ catalyst support is hydrophilic but ZrO₂ is weakly hydrophilic and the usage of ZrO₂ as a co-support will be beneficial for the desorption of produced H₂O from the CO₂ hydrogenation reaction [6]. Zhang et al. [15] reported that addition of up to 15 wt% ZrO₂ into γ -Al₂O₃ improved the dispersion of CuO species and enhanced the catalytic performance in the CO₂ hydrogenation reaction.

In the present study, we report the synthesis of Cu/ZnO on mixed oxide support comprising Al₂O₃ and ZrO₂ using the impregnation method. To the best of our knowledge, the effects of calcination conditions on the catalytic performance for CO₂ hydrogenation reaction over Cu/ZnO catalyst supported on Al₂O₃-ZrO₂ has not been reported. In the present contribution, the influence of calcination conditions of the promoted Cu/ZnO/Al₂O₃-ZrO₂ catalyst on their catalytic activity in CO₂ hydrogenation is systematically studied via response surface methodology (RSM) with rotatable central composite design (CCD).

2. Results and Discussion

2.1. Model Fitting

Three independent variables for the calcination process (temperature, ramping rate, and duration) at different levels were investigated in this study. An experimental design was constructed and analyzed using Design Expert Version 10 (Stat Ease, Minneapolis, MN, USA) in order to find the optimum point of the calcination condition for the synthesized catalyst (MNCZAZ). Optimization of the calcination conditions (calcination temperature, ramping rate, and duration) were carried out with rotational central composite design (CCD), which is the best DOE that applies RSM [16]. CCD is the experimental design introduced by Box and Wilson in 1951. CCD is one of the best experimental designs used in RSM. However, this design requires selection of the correct type of CCD. The CCD types include spherical (SCCD), rotatable (RCCD), orthogonal (OCCD), and face-centered (FCCD) central composite. In this study, the RCCD approach was used to determine the interaction between the process variables and the process response. According to previous research, the common type of CCD is either face-centered or rotatable [17]. One of the reasons for choosing rotatable CCD is the ability to perform extreme analysis in DOE compared to face-centered CCD. Therefore, the studied range would be much wider and more reliable to observe the trends.

The number of tests needed for RCCD includes the standard 2k factorial with the origin at the center, 2k points fixed axially at a distance, say θ , from the center to generate the quadratic terms, and retests at the center; where k is the number of variables [18]. The axial points are chosen to be rotatable, which ensures that the variance of the model prediction is constant at all points equidistant from the design center. Repeats of the test at the center are very important as they provide an independent estimate of the experimental error [19]. For three variables, the recommended number of trials at the center is six. Therefore, the total number of trials required for these three independent variables is $2^3 + (2 \times 3) + 6 = 20$ [19,20]. Once the desired ranges of values of the variables are defined, they are coded to be ± 1 for the factorial points, 0 for the midpoints, and $\pm\alpha$ for the axial points. The codes are computed as functions of the range of interest of each factor, as shown in Table 1. Table 2 shows the design matrix for the study on calcination conditions and the measured responses (CO₂ conversion, methanol selectivity, and methanol yield).

Table 1. Independent variables in Experimental Design.

Variables	Unit	Levels				
		− α Min	−1 Low	0 Mid	1 High	+ α Max
A: Calcination temperature	°C	181	250	350	450	518
B: Ramping rate	°C/min	1	5	17.5	30	40
C: Duration (h)	h	1	2	4	6	7

Table 2. Experimental design matrix for MNCZAZ calcination condition.

Run	A	B	C	Response 1: X_{CO_2}	Response 2: S_{MEOH}	Yield _{MEOH}
1	350	17.5	4	16.02	75.86	12.15
2	518	17.5	4	7.19	58.35	4.19
3	450	5	6	3.35	52.39	1.75
4	250	30	6	5.55	25.43	1.41
5	250	5	2	8.17	20.91	1.70
6	250	30	2	7.97	47.59	3.79
7	450	30	2	7.43	63.83	4.74
8	350	17.5	1	5.55	47.76	2.65
9	250	5	6	7.87	5.57	0.43
10	350	1	4	15.81	68.77	10.87
11	350	17.5	4	13.6	63.1	8.58
12	350	17.5	4	15.9	74	11.76
13	350	17.5	4	16.01	75	12.00
14	350	40	4	9.63	52.54	5.05
15	350	17.5	4	16.04	76.1	12.2
16	450	30	6	11.28	37.34	4.21
17	350	17.5	4	16.1	75.1	12.09
18	181	17.5	4	6.47	19.52	1.26
19	350	17.5	7	7.91	24.63	1.94
20	450	5	2	5.75	42.46	2.44

The CO_2 conversion, X_{CO_2} , and methanol selectivity, S_{MEOH} , were taken as the response variables of the designed experiments. The design of experiment was tabulated in Table 2 and the experimental data were then modeled using polynomial Equation (1) (CO_2 conversion) and Equation (2) (methanol selectivity).

$$X_{CO_2} = 15.84 - 0.052A + 0.38B + 0.18C + 1.52AB + 0.52AC + 0.52BC - 3.10 A^2 - 1.80B^2 - 3.92C^2 \quad (1)$$

$$S_{MEOH} = 74.09 + 11.79A + 4.92B - 7.10C - 5.03AB + 2.62BC - 5.40BC - 12.25 A^2 - 8.45B^2 - 16.67C^2 \quad (2)$$

2.2. Regression Model Equation and Analysis of Variance (ANOVA)

To determine the best model for both responses, the proposed model should be considered as a favorable beginning [21]. The proposed model by the software is the quadratic model, which shows that both models are adequately sufficient to describe the calcination condition within the experimental range.

As shown in Table 3 for first response parameter, X_{CO_2} , the quadratic model is suggested with high significance at a 5% confidence level as indicated by low p -value < 0.0001 . On the other hand, the insignificant lack of fit (LOF) value (0.0711), of this study indicates that the model is a good representation of the response as the probability for lack of fit describes the variation of the data around the fitted model. The determination coefficient (R^2) values which measures the fitness of the data with the model is at 93%, suggesting that the model is significant with R^2 value and adjusted R^2 of 0.93 and 0.87, respectively. The value is acceptable because it is very close to unity. The R^2 value illustrate the closeness of the selected model to the experimental data points. Meanwhile, the adjusted R^2 describes the

amount of variation about the mean explained by the model [21]. Furthermore, adequate precision values of the model also show a value higher than 4, which is desirable for the design with value of 15.31.

For a second response, S_{MEOH} , the model is also proved to be significant with R^2 value up to 0.96 and LOF of 0.2813.

Table 3. Analysis of variance (ANOVA) for the calcination study of MNCZAZ.

Model	X_{CO_2}	S_{MEOH}
	Quadratic Model	Quadratic Model
Standard deviation	1.59	5.84
R^2	0.93	0.96
Adjusted R^2	0.87	0.93
Adequate precision	9.75	15.36
p -value	<0.0001	<0.0001
F-value	15.31	28.86
LOF	0.0711	0.2813

Multiple regression coefficient of a second order polynomial model describing the effect of catalyst (MNCZAZ) calcination conditions on the values of X_{CO_2} and S_{MEOH} are summarized in Tables 4 and 5, respectively. The significance of each coefficient was determined by F-value and p -value. The p -value is considered as significant if the value is less than 0.05. For the calcination condition effect of the catalyst (MNCZAZ) on X_{CO_2} , the interaction between first order effect of A (temperature) and B (ramping rate) are significant at p value of 0.0224 while the other interactions are not significant ($p > 0.05$). Furthermore, the second order effect of A (temperature) and C (duration) are also significant with p -value of <0.0001. The same trend is also observed with second order effect of B (ramping rate) with p -value = 0.0044. The coefficient estimate values of the regression model are A = 0.052 (temperature), B = 0.38 (ramping rate), and C = 0.18 (duration). Therefore, ramping rate has the highest effect on the response X_{CO_2} , followed by duration and temperature, summarized as $B > C > A$.

Table 4. Coefficient of regression model and their significance for first response, X_{CO_2} .

Source	Coefficient Estimate	F-Value	Prob. > F	Remarks
Quadratic model		15.31	<0.0001	significant
A	−0.052	0.015	0.9063	insignificant
B	0.38	0.61	0.4545	insignificant
C	0.18	0.16	0.6949	insignificant
AB	1.52	7.27	0.0224	significant
AC	0.52	0.86	0.3758	insignificant
BC	0.52	0.84	0.3802	insignificant
A^2	−3.10	55.75	<0.0001	significant
B^2	−1.80	13.41	0.0044	significant
C^2	−3.90	62.38	<0.0001	significant

Effects of catalyst (MNCZAZ) calcination conditions on the second response, S_{MEOH} , are shown in Table 5. All three first order effects of A (temperature), B (heating ramp), and C (heating duration) are significant with p -value of <0.0001, 0.0208, and 0.0016, respectively. The interaction between the first order effect of AB and BC are also significant with p -value of 0.0352 and 0.0257, respectively. In addition, the second order effect of A, B, and C are also significant with p -values ≤ 0.0009 . The coefficient estimate values of the S_{MEOH} regression model are A = 11.79 (temperature), C = 7.10 (duration), and B = 4.92 (ramping rate).

Based on the corresponding p -value, the first order effect of B is least significant amongst the variables studied as it has lowest coefficient estimation. Therefore, temperature

has the highest effect to the response S_{MEOH} , followed by duration and ramping rate, summarized as $A > C > B$.

Table 5. Coefficient of regression model and their significance for second response, S_{MEOH} .

Source	Coefficient Estimate	F-Value	Prob. > F	Remarks
Quadratic model		28.86	<0.0001	significant
A	11.79	55.74	<0.0001	significant
B	4.92	7.51	0.0208	significant
C	-7.10	18.48	0.0016	significant
AB	-5.03	5.93	0.0352	significant
AC	2.62	1.61	0.2336	insignificant
BC	-5.40	6.85	0.0257	significant
A ²	-12.25	64.72	<0.0001	significant
B ²	-8.45	21.84	0.0009	significant
C ²	-16.67	83.45	<0.0001	significant

2.3. Interaction Effect of Calcination Condition of Catalyst (MNCZAZ)

The optimum response and the relationship between significant model terms are illustrated in Figures 1–6 which exhibit the 3-D curvature and its respective contour plots for:

1. temperature and ramping rate (AB)
2. temperature and duration (AC)
3. ramping rate and duration (BC)

These are the three possible two-factor combination interactions for studying the effects of catalyst (MNCZAZ) calcination conditions on the values of X_{CO_2} and S_{MEOH} .

Figure 1 shows the simultaneous effects of A and B variables which have the most significant influence on the CO_2 conversion (X_{CO_2}). The values of X_{CO_2} increased when A and B were increased from 181–350 ($^{\circ}\text{C}$) and 5–17.5 ($^{\circ}\text{C}/\text{min}$), respectively. Increasing the calcination temperature further to 450 and 518 ($^{\circ}\text{C}$) caused X_{CO_2} to decrease significantly by 10–13% from that of the highest value (16.01%). The same trend was observed when the calcination temperature was decreased from 250 to 181 ($^{\circ}\text{C}$).

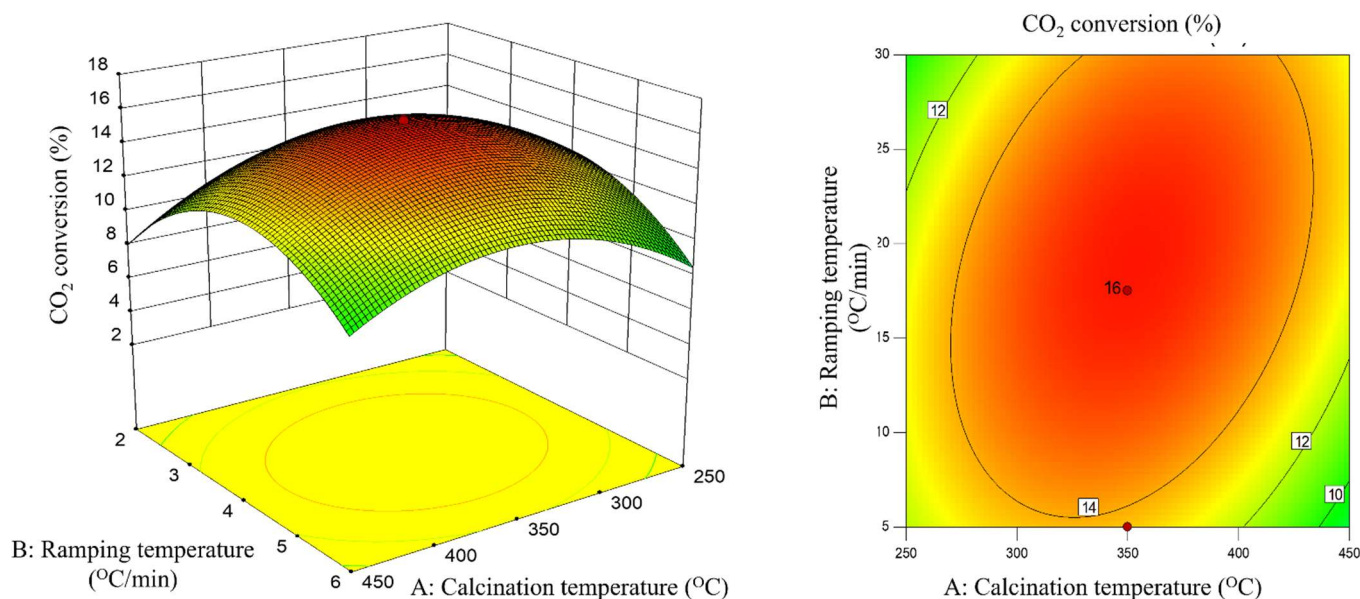


Figure 1. Interaction effects of AB on CO_2 conversion.

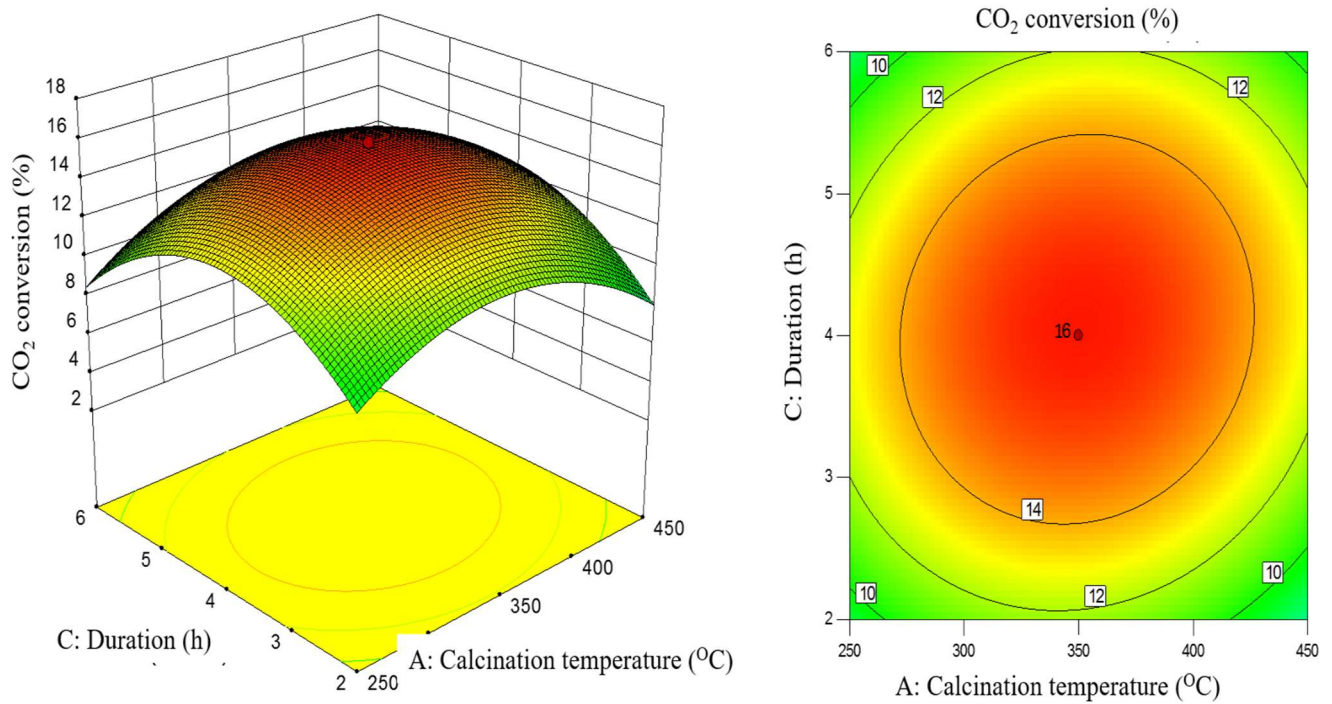


Figure 2. Interaction effects of AC on CO₂ conversion.

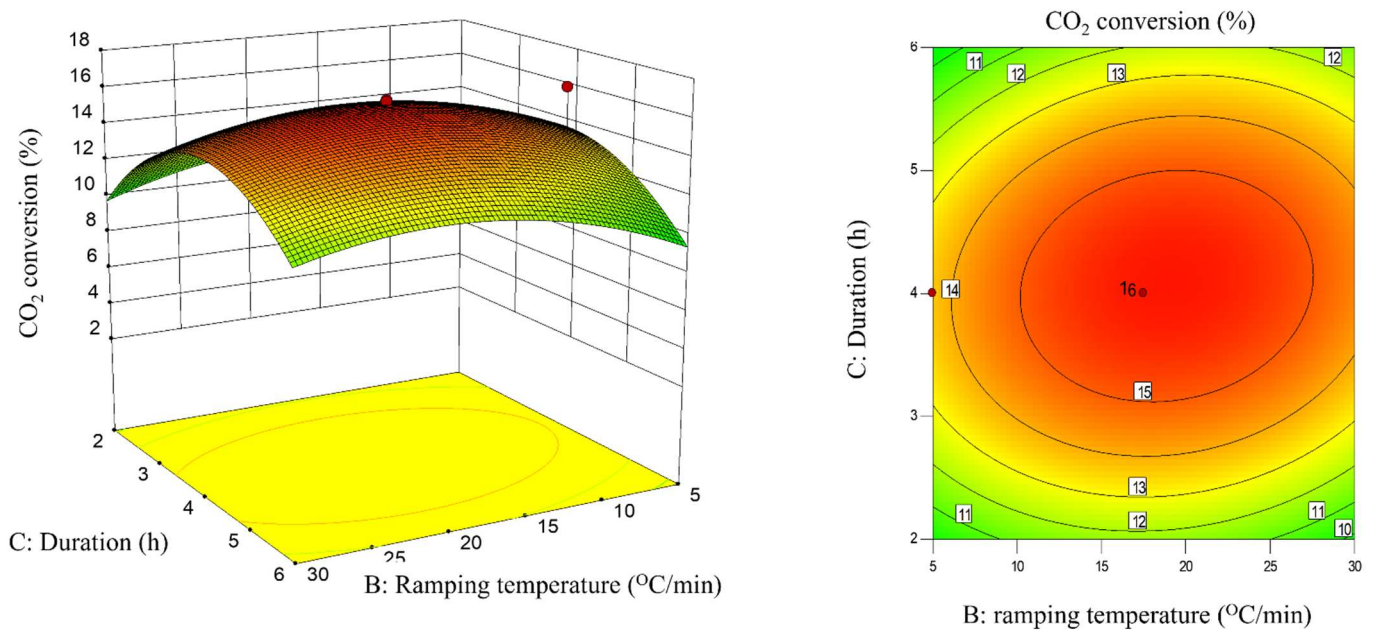


Figure 3. Interaction effects of BC for CO₂ conversion.

Interaction effects of AB and AC on methanol selectivity are depicted in Figures 4 and 5, respectively. Figure 6 shows the simultaneous effects of B and C, which exhibit the most significant influence on methanol selectivity, (S_{MEOH}) study. The selectivity to methanol was maximized when B was at the center point at 17.5 °C/min and C was increased from 1–4 (h). Increasing or decreasing the ramping rate of 17.5 (°C/min) and duration longer than 4 h caused the S_{MEOH} to decrease significantly by 70–90% from the highest value of 75.86%.

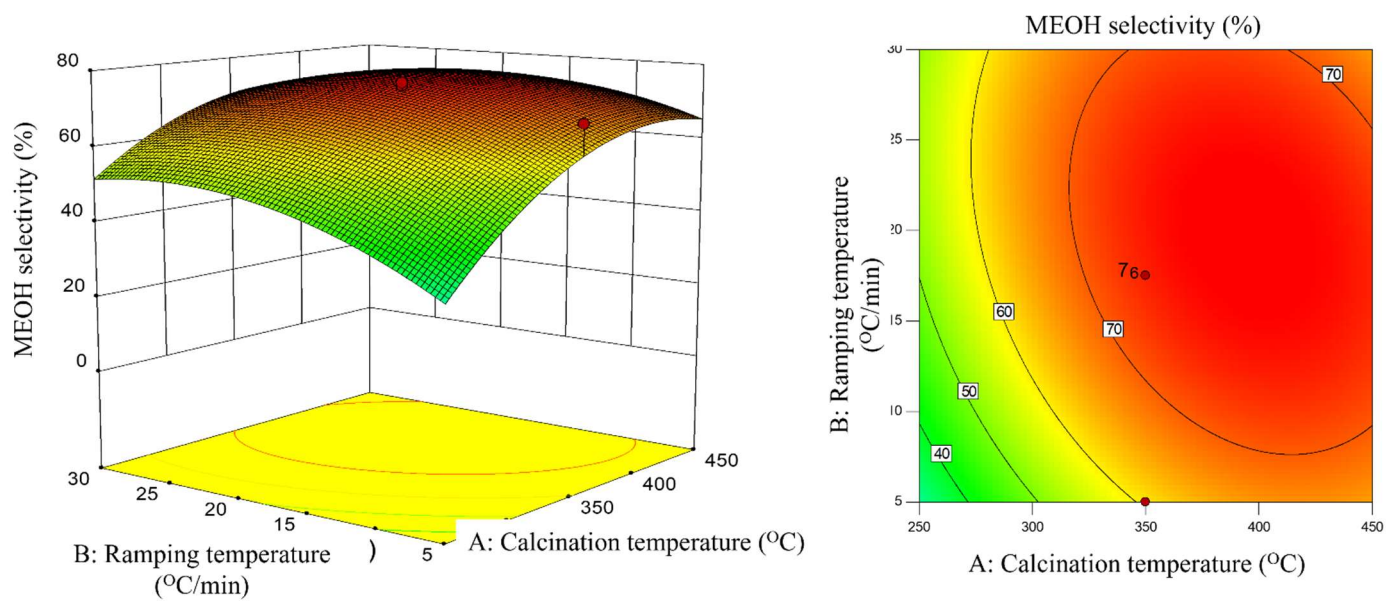


Figure 4. Interaction Effect of AB for methanol selectivity.

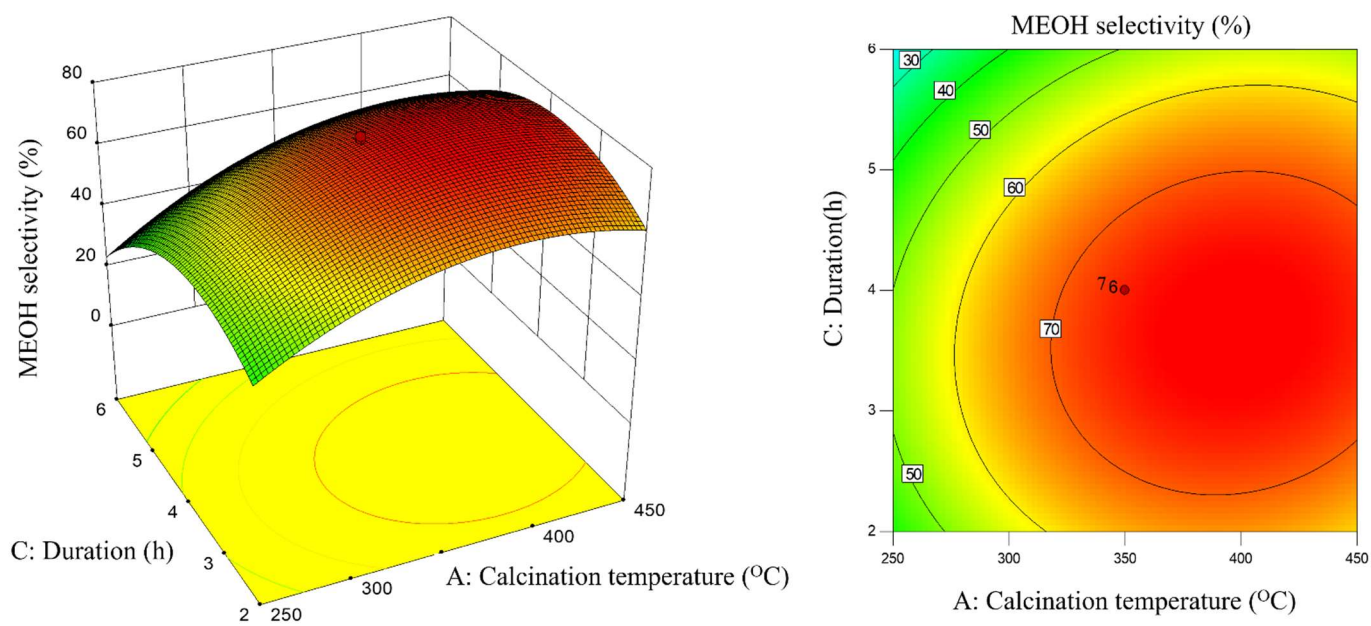


Figure 5. Interaction Effect of AC for methanol selectivity.

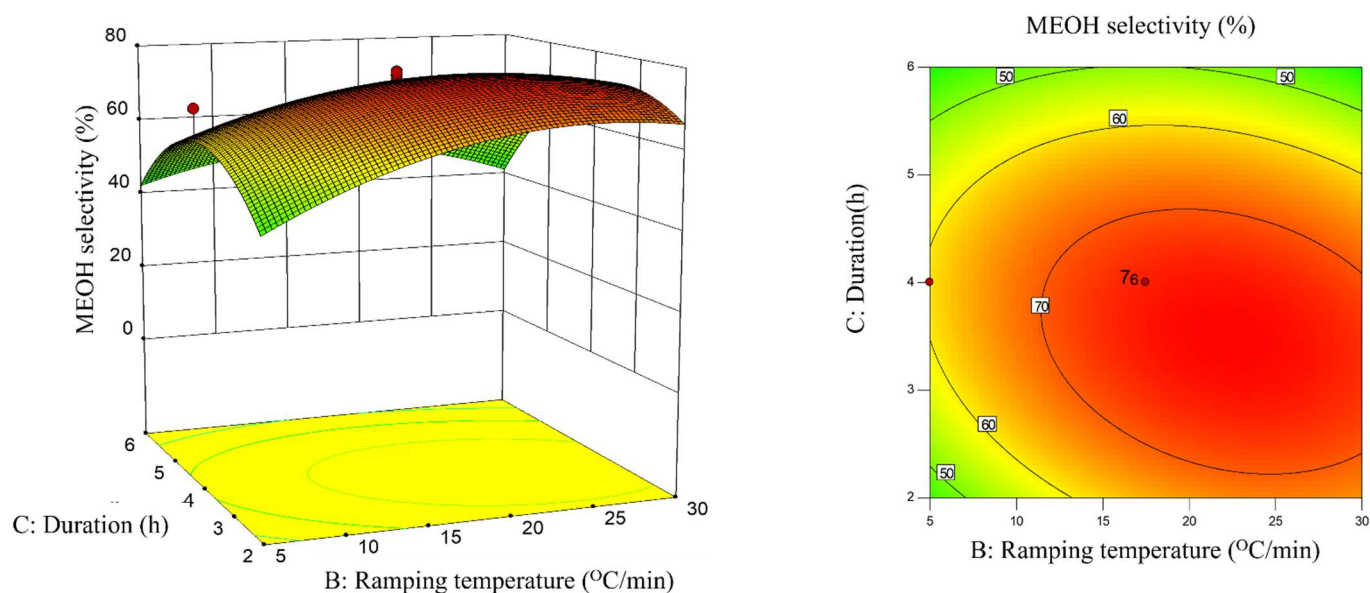


Figure 6. Interaction Effect of BC for methanol selectivity.

2.4. Diagnostic Plots of the Calcination Parameters to X_{CO_2} and S_{MEOH} Responses

Residual analysis was applied to both models for adequacy inspection to avoid any inadequate fit of the approximating model. The normal probability plots shown in Figures 7 and 8a implied that the experimental data fitted well to the straight lines. These trends indicated normal distribution of the data, thus confirming the normality of the experimental data. The qualification of fit data plots, shown in Figures 7 and 8b, further confirmed good representation of the established polynomial model. The statement was validated as the actual data points fell near the straight line within acceptable variance range, when compared to the calculated value [22]. Based on this analysis, the optimal calcination condition for the catalyst (MNCZAZ) was then calculated using Equation (1) for X_{CO_2} and Equation (2) for S_{MEOH} experiments. To summarize, the analysis agreed with the experimental data where the difference between the calculated and experimental optimal point for X_{CO_2} and S_{MEOH} was only 4.32 and 2.81%, respectively (Table 6).

Table 6. Optimum conditions for the synthesized catalyst (MNCZAZ).

Variables	Units	Optimum Conditions
A	°C	342
B	°C/min	17.9
C	h	4
X_{CO_2} activity, calculated	%	16.2
X_{CO_2} activity, experimental	%	15.5
Percentage error, X_{CO_2}	%	4.32
S_{MEOH} activity, calculated	%	74.7
S_{MEOH} activity, experimental	%	72.6
Percentage error, S_{MEOH}	%	2.81
Standard deviation	%	1.01

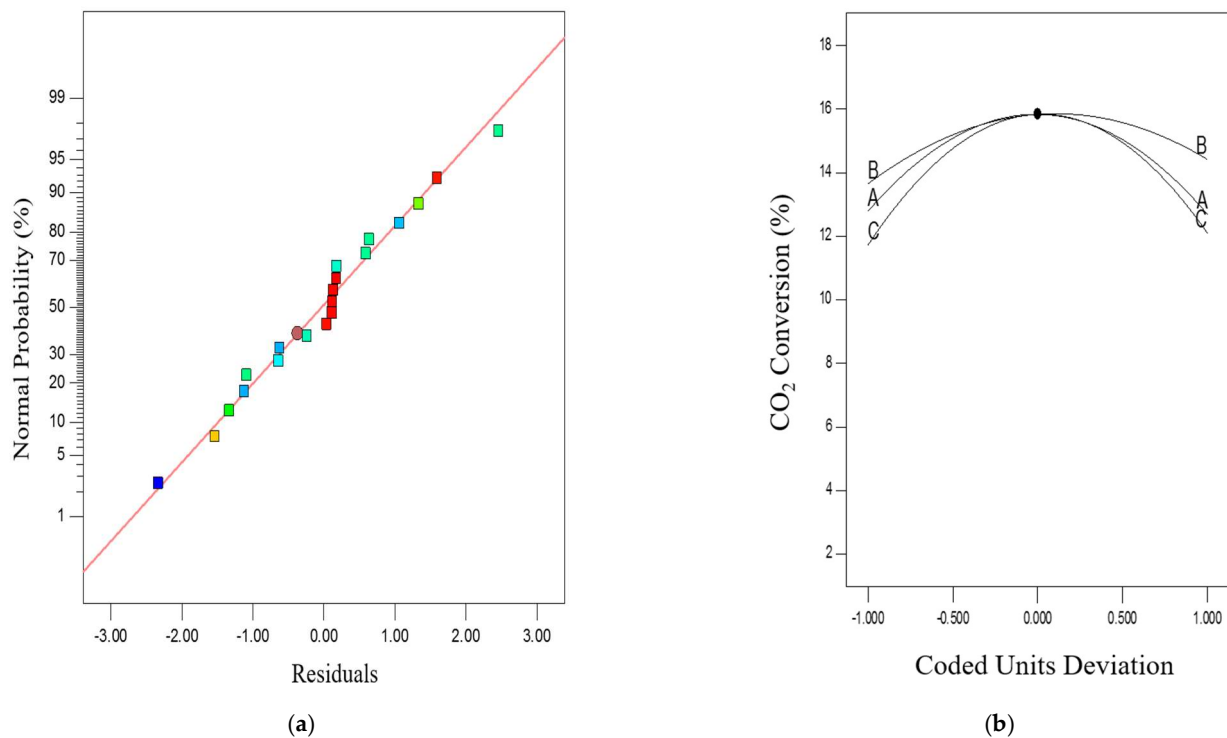


Figure 7. CO₂ conversion (a) normal probability plot (b) quality of fit data.

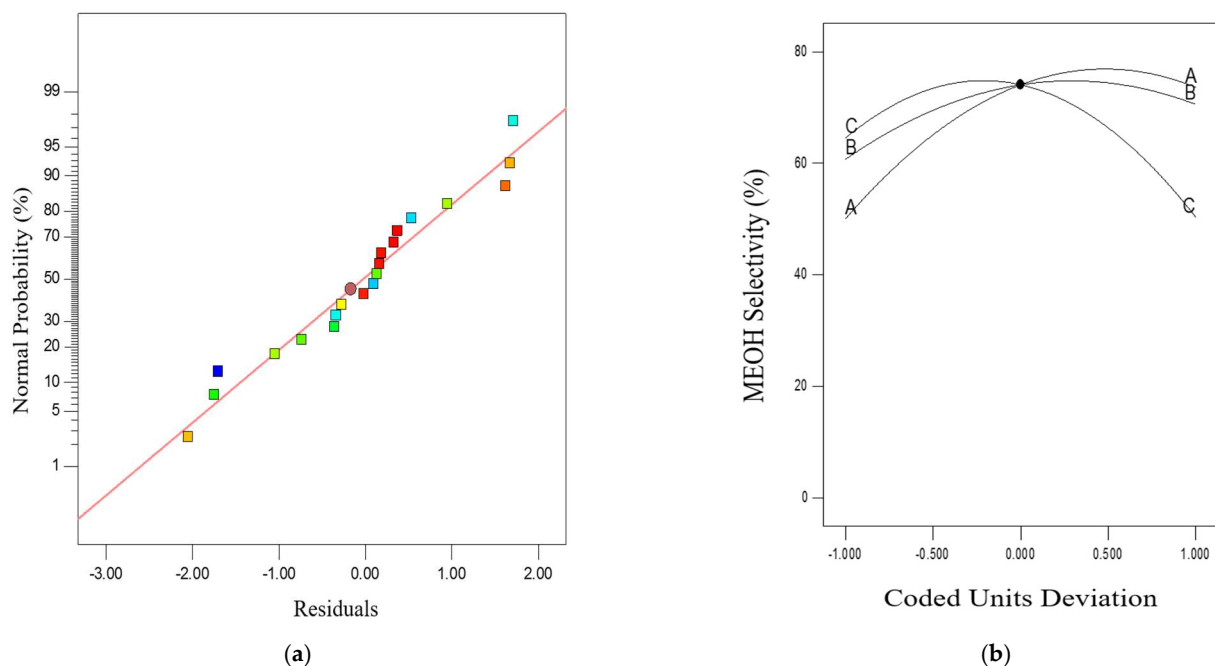


Figure 8. Methanol Selectivity (a) normal probability plot (b) quality of fit data.

2.5. RSM Optimizations of Calcination Parameters

The main objective of RSM is to determine the optimum condition for the process. From the analysis, the optimum calcination parameters for CO₂ hydrogenation activity of the synthesized catalyst (MNCZAZ) are summarized in Table 6. The selected optimum conditions were based on the maximum X_{CO_2} and S_{MEOH} and its desirability, which is 1.000. Using the same experimental method, three confirmation runs were conducted to validate the results. The calculated X_{CO_2} and S_{MEOH} activity differences with experimental

values were approximately 0.7% to 2.1%, respectively. The percentage errors difference between the calculated and experimental values were within the acceptable value of 5%. Thus, these repeated optimized runs further confirmed the reliability of the regression equation model.

2.6. Textural and Morphological Properties

Figure 9 shows the field-emission scanning electron microscopy (FESEM) image and the elemental maps of the Cu, Zn, Al, Zr of the MNCZAZ catalyst. This elemental map shows that both CuO and ZnO were dispersed on the Al₂O₃-ZrO₂ support with slight agglomeration on the surface (represented by the scattered green and yellow spots).

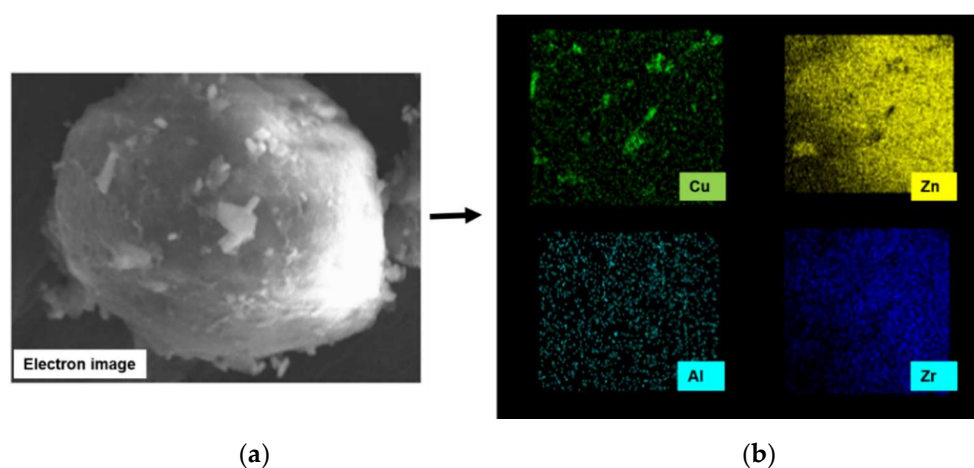


Figure 9. (a) FESEM image (b) Elemental mapping of MNCZAZ catalyst obtained by energy dispersive X-ray (FESEM/EDX).

Table 7 shows the impregnated elemental composition of the catalyst, as determined by X-Ray fluorescence (XRF) technique. The compositions of Cu and Zn as well the Mn and Nb promoters were found to be in good agreement with the theoretical values.

Table 7. Elemental Composition of MNCZAZ as measured by XRF.

Weight (%)			
Cu	Zn	Mn	Nb
11.27	3.72	0.05	0.04

Table 8 shows the textural properties of some of the catalysts which were calcined under various conditions. The data were arranged from the highest to the lowest calcination temperature. The results of ANOVA indicated that calcination temperature had the highest effect to the methanol selectivity. The BET surface areas and pore diameters of the catalyst were found to be influenced by the calcination temperature. The BET surface area increased from 137 m²/g to 167 m²/g as the calcination temperature decreased from 518 °C to 181 °C at the same condition of 17.5 °C /min ramping rate and 4 h duration. An opposite trend was observed for the pore diameter which decreased from 8.9 nm to 7.4 nm when the calcination temperature decreased from 518 to 181 °C. Near the optimum calcination condition, the catalyst exhibited a BET surface area of 147 m²/g, a pore volume of 0.31 cm³/g, and a pore diameter of 8.1 nm, which resulted in the highest methanol selectivity.

Table 8. Textural properties of catalysts calcined under different conditions.

Temperature (°C)	Ramping Rate (°C/min)	Duration (h)	S _{BET} (m ² /g)	V _p (cm ³ /g)	D _{BJH} (nm)	X _{CO₂} (%)	S _{MeOH} (%)
518	17.5	4	137	0.31	8.9	7.19	58.35
450	5	6	143	0.31	8.6	3.35	52.39
350	10	4	140	0.31	6.2	15.81	68.77
350	17.5	4	147	0.31	8.1	16.02	75.86
250	5	6	123	0.24	7.6	7.87	5.57
181	17.5	4	167	0.31	7.4	6.47	19.52

S_{BET} is BET surface area; V_p is pore volume; and D_{BJH} is the BJH pore diameter.

3. Materials and Methods

3.1. Experimental Design

A standard response surface methodology (RSM) design, also known as central composite design (CCD), was used to study the calcination parameters of the synthesized Cu-based catalyst (MNCZAZ) for CO₂ hydrogenation reaction. The calcination parameters investigated were the temperature, ramping rate, and duration. An empirical model was developed to correlate the response X_{CO₂} and S_{MeOH} to the three respective parameters affecting the CO₂ hydrogenation process in methanol synthesis by using a second-degree polynomial equation, as given by the following equation.

$$\gamma = \beta_0 + \beta_1 A + \beta_2 B + \beta_3 C + \beta_{12} AB + \beta_{13} AC + \beta_{23} BC + \beta_{11} A^2 + \beta_{22} B^2 + \beta_{33} C^2 \quad (3)$$

where γ is the predicted response; β_0 is the constant coefficient; β_1, β_2 and β_3 are the linear coefficients; β_{12}, β_{13} , and β_{23} are the interaction coefficients; β_{11}, β_{22} , and β_{33} are the quadratic coefficients; and A, B, C are the coded values of independent input parameters.

To correlate between all responses and analyze the experimental condition with the highest desirability, Design Expert Version 10 (Stat Ease, Minneapolis, MN, USA) was utilized. Analysis of variance (ANOVA) explained every variation in the statistically obtained model and illustrates the importance of each model parameter. The F-test for a confidence level of 95% as well as the lack of fit (LOF) test was used to evaluate the significance of the model. Typically, the model is classified as more significant when it shows greater F-value and smaller *p*-value.

3.2. Preparation and Characterization of MNCZAZ Catalyst

To synthesize 10 g MNCZAZ catalyst, 0.021 g of Mn(NO₃)₂·4H₂O [Merck, Subang Jaya, Malaysia], 0.014 g of C₄H₄NNbO₉ [Merck, Malaysia], 3.995 g of Cu(NO₃)₂ [Merck, Malaysia], and 1.644 g of Zn(NO₃)₂ [Sigma Aldrich, Malaysia], were stirred for 1 h in deionized water then added drop wisely onto the Al₂O₃-ZrO₂ [SASOL, Hamburg, Germany] powder. The composition of the mixed support was 80 wt% Al₂O₃ and 20 wt% ZrO₂. The slurry was continuously stirred for 24 h at pH 7 using 10% ammonia solution, NH₄OH [Merck, Malaysia] to maintain the pH. The mixture was filtered and dried at 120 °C for 12 h and then calcined in air under the calcination conditions listed in Table 2.

The surface morphology of the synthesized samples was observed on a Hitachi-8020 field-emission scanning electron microscope (FESEM/EDX) (Hitachi High-Technologies Corporation, Tokyo, Japan) The textural properties were obtained via nitrogen adsorption-desorption isotherms measured on a Micromeritics ASAP 2020 adsorption analyzer (Micromeritics Instrument Corporation, Norcross, GA, USA) Metal contents were determined by X-ray fluorescence using a Bruker S8 Tiger X-ray Spectrometer (Bruker, Wissembourg, France).

3.3. Catalytic Performance Evaluation of MNCZAZ Catalyst

Catalytic activity evaluation was performed in a stainless-steel fixed-bed reactor (Microactivity Reference, PID Eng Tech, Norcross, GA, USA). A 0.2 g sample was reduced in situ by pure H₂ flowing at 20 mL min⁻¹ for 2 h prior to the hydrogenation process. Then, CO₂ hydrogenation reaction was performed on the reduced catalyst at 22.5 bar, 250 °C, and CO₂: H₂ (1:3) with a total flow rate of 36 mL/min for 5 h. The reaction condition was fixed for all the catalysts synthesized according to the design matrix (Table 2). A gas chromatograph (Agilent 7890A) equipped with a TCD detector for H₂ and CO₂ analysis, and an FID detector for analysis of alcohols and other hydrocarbons, were used to analyze the reactor effluents [23]. CO₂ conversion, methanol selectivity, and methanol yield were calculated using Equations (4)–(6), respectively.

$$\text{CO}_2 \text{ conversion (\%)} = \frac{\text{Mole of CO}_2 \text{ in} - \text{Mole of CO}_2 \text{ out}}{\text{Mole of CO}_2 \text{ in}} \times 100 \quad (4)$$

$$\text{Methanol selectivity (\%)} = \frac{\text{mole of methanol produced}}{\text{total mole of product}} \times 100 \quad (5)$$

$$\text{Methanol yield (\%)} = \frac{\text{CO}_2 \text{ conversion (\%)}}{100} \times \text{Methanol selectivity (\%)} \quad (6)$$

4. Conclusions

In conclusion, the calcination conditions of Cu-based catalysts for methanol synthesis through CO₂ hydrogenation process was optimized using RCCD of RSM. Quadratic model was proposed to correlate the experimental variables for both CO₂ conversion (X_{CO_2}) and methanol selectivity (S_{MEOH}) responses. It was found that the model was able to predict the experimental data to high accuracy for X_{CO_2} and S_{MEOH} with R^2 of 0.93 and 0.96, respectively. The interactions among the calcination temperature, A, and ramping rate, B, were found to have the most significant effect on the CO₂ conversion; meanwhile, the calcination's ramping rate and duration (B and C) had a significant effect on the methanol selectivity. The optimization of calcination conditions was studied and the computed values by the models were found to be in good agreement with the experimental values. The optimum calcination condition for a Mn/Nb-promoted Cu/ZnO/Al₂O₃-ZrO₂ catalyst (MNCZAZ) for a CO₂ hydrogenation reaction to produce methanol is at 342 °C, with a ramping rate of 17.9 °C per min for 4 h. Confirmatory experiments were conducted to evaluate the accuracy of the optimized conditions and the findings show that the range of deviation was 1.01%.

Author Contributions: Conceptualization, N.A.M.Z. and S.F.H.T.; methodology, N.H.B. and N.I.Z.; formal analysis, N.I.Z.; writing-review and editing, N.I.Z., N.H.B. and N.A.M.Z.; visualization, N.I.Z.; supervision, N.A.M.Z.; funding acquisition, N.A.M.Z. and S.F.H.T. All authors have read and agreed to the published version of the manuscript.

Funding: This research was funded by International Collaborative Research Fund, (Cost center: 015ME0-207).

Acknowledgments: Research support received from Universiti Teknologi PETRONAS and American University of Ras Al Khaimah are gratefully acknowledged.

Conflicts of Interest: The authors declare no conflict of interest.

References

1. Atsbha, T.A.; Yoon, T.; Seongho, P.; Lee, C.J. A review on the catalytic conversion of CO₂ using H₂ for synthesis of CO, methanol, and hydrocarbons. *J. CO₂ Util.* **2021**, *44*, 101413. [\[CrossRef\]](#)
2. Zhang, X.; Zhang, G.; Liu, W.; Yuan, F.; Wang, J.; Zhu, J.; Jiang, X.; Zhang, A.; Ding, F.; Song, C.; et al. Reaction-driven surface reconstruction of ZnAl₂O₄ boosts the methanol selectivity in CO₂ catalytic hydrogenation. *Appl. Catal. B Environ.* **2021**, *284*, 119700. [\[CrossRef\]](#)

3. Alsuhaibani, A.S.; Afzal, S.; Challiwala, M.; Elbashir, N.O.; El-Halwagi, M.M. The impact of the development of catalyst and reaction system of the methanol synthesis stage on the overall profitability of the entire plant: A techno-economic study. *Catal. Today* **2020**, *343*, 191–198. [[CrossRef](#)]
4. Vita, A.; Italiano, C.; Pino, L.; Laganà, M.; Ferraro, M.; Antonucci, V. High-temperature CO₂ methanation over structured Ni/GDC catalysts: Performance and scale-up for Power-to-Gas application. *Fuel Process. Technol.* **2020**, *202*, 106365. [[CrossRef](#)]
5. Ren, S.; Fan, X.; Shang, Z.; Shoemaker, W.R.; Ma, L.; Wu, T.; Li, S.; Klinghoffer, N.B.; Yu, M.; Liang, X. Enhanced catalytic performance of Zr modified CuO/ZnO/Al₂O₃ catalyst for methanol and DME synthesis via CO₂ hydrogenation. *J. CO₂ Util.* **2020**, *36*, 82–95. [[CrossRef](#)]
6. Li, K.; Chen, J.G. CO₂ Hydrogenation to Methanol over ZrO₂-Containing Catalysts: Insights into ZrO₂ Induced Synergy. *ACS Catal.* **2019**, *9*, 7840–7861. [[CrossRef](#)]
7. Marcos, F.C.; Lin, L.; Betancourt, L.E.; Senanayake, S.D.; Rodriguez, J.A.; Assaf, J.M.; Giudici, R.; Assaf, E.M. Insights into the methanol synthesis mechanism via CO₂ hydrogenation over Cu-ZnO-ZrO₂ catalysts: Effects of surfactant/Cu-Zn-Zr molar ratio. *J. CO₂ Util.* **2020**, *41*, 101215. [[CrossRef](#)]
8. Wu, J.; Saito, M.; Takeuchi, M.; Watanabe, T. The stability of Cu/ZnO-based catalysts in methanol synthesis from a CO₂-rich feed and from a CO-rich feed. *Appl. Catal. A Gen.* **2001**, *218*, 235–240. [[CrossRef](#)]
9. Din, I.U.; Usman, M.; Khan, S.; Helal, A.; Alotaibi, M.A.; Alharthi, A.I.; Centi, G. Prospects for a green methanol thermo-catalytic process from CO₂ by using MOFs based materials: A mini-review. *J. CO₂ Util.* **2021**, *43*, 101361. [[CrossRef](#)]
10. Mureddu, M.; Lai, S.; Atzori, L.; Rombi, E.; Ferrara, F.; Pettinau, A.; Cutrufello, M.G. Ex-LDH-based catalysts for CO₂ conversion to methanol and dimethyl ether. *Catalysts* **2021**, *11*, 615. [[CrossRef](#)]
11. Duyar, M.S.; Gallo, A.; Regli, S.K.; Snider, J.L.; Singh, J.A.; Valle, E.; McEnaney, J.; Bent, S.F.; Rønning, M.; Jaramillo, T.F. Understanding selectivity in CO₂ hydrogenation to methanol for mop nanoparticle catalysts using in situ techniques. *Catalysts* **2021**, *11*, 143. [[CrossRef](#)]
12. Bibi, M.; Ullah, R.; Sadiq, M.; Sadiq, S.; Khan, I.; Saeed, K.; Zia, M.A.; Iqbal, Z.; Ullah, I.; Iqbal, Z.; et al. Catalytic hydrogenation of carbon dioxide over magnetic nanoparticles: Modification in fixed-bed reactor. *Catalysts* **2021**, *11*, 592. [[CrossRef](#)]
13. Lu, Z.; Sun, K.; Wang, J.; Zhang, Z.; Liu, C. A Highly Active Au/In₂O₃-ZrO₂ Catalyst for Selective Hydrogenation of CO₂ to Methanol. *Catalysts* **2020**, *11*, 1360. [[CrossRef](#)]
14. Fujita, S.I.; Moribe, S.; Kanamori, Y.; Kakudate, M.; Takezawa, N. Preparation of a coprecipitated Cu/ZnO catalyst for the methanol synthesis from CO₂- effects of the calcination and reduction conditions on the catalytic performance. *Appl. Catal. A Gen.* **2001**, *207*, 121–128. [[CrossRef](#)]
15. Zhang, Y.; Fei, J.; Yu, Y.; Zheng, X. Methanol synthesis from CO₂ hydrogenation over Cu based catalyst supported on zirconia modified γ -Al₂O₃. *Energy Convers. Manag.* **2006**, *47*, 3360–3367. [[CrossRef](#)]
16. Amin, N.A.S.; Zakaria, Z.Y. Optimization of Oxidative Coupling of Methane Using Response Surface Methodology. *J. Teknol.* **2012**, *39*, 35–51.
17. Eze, F.C.; Ngonadi, L. Alphabetic Optimality Criteria for 2K Central Composite Design. *App. Math. Sci.* **2018**, *4*, 107–118.
18. Aslan, N. Application of response surface methodology and central composite rotatable design for modeling and optimization of a multi-gravity separator for chromite concentration. *Powder Technol.* **2008**, *185*, 80–86. [[CrossRef](#)]
19. Box, G.E.P.; Hunter, J.S. Multi-Factor Experimental Designs for Exploring Response Surfaces. *Ann. Math. Stat.* **1957**, *28*, 195–241. [[CrossRef](#)]
20. Obeng, D.P.; Morrell, S.; Napier-Munn, T.J. Application of central composite rotatable design to modelling the effect of some operating variables on the performance of the three-product cyclone. *Int. J. Miner. Process.* **2005**, *76*, 181–192. [[CrossRef](#)]
21. Anuar, M.A.M.; Amran, N.A.; Ruslan, M.S.H. Optimization of Progressive Freezing for Residual Oil Recovery from a Palm Oil – Water Mixture (POME Model). *ACS Omega* **2020**, *6*, 2707–2716. [[CrossRef](#)] [[PubMed](#)]
22. Saafie, N.; Samsudin, M.R.; Sufian, S. Optimization of methylene blue adsorption via functionalized activated carbon using response surface methodology with central composite design. *Key Eng. Mater.* **2020**, *841*, 220–224. [[CrossRef](#)]
23. Tasfy, S.F.H.; Mohd Zabidi, N.A.; Shaharun, M.S.; Subbarao, D. Effect of Mn and Pb Promoters on the Performance of Cu/ZnO-Catalyst in CO₂ Hydrogenation to Methanol. *Appl. Mech. Mater.* **2014**, *625*, 289–292. [[CrossRef](#)]